EPJ manuscript No.
(will be inserted by the editor)

An Introduction to the Hydrodynamics of Swimming Microorganisms

Julia M. Yeomans[1,a], Dmitri O. Pushkin[1], and Henry Shum[2]

[1] Rudolf Peierls Centre for Theoretical Physics, University of Oxford, 1 Keble Road, Oxford OX1 3NP, UK
[2] Department of Chemical & Petroleum Engineering, University of Pittsburgh, 1249 Benedum Hall, Pittsburgh, PA 15261, USA

Abstract. This manuscript is a summary of a set of lectures given at the Geilo School 2013 *Soft Matter Confinement: from Biology to Physics*. It aims to provide an introduction to the hydrodynamics that underlies the way in which microorganisms, such as bacteria and algae, and fabricated microswimmers, swim. We focus on two features peculiar to bacterial swimming: the Scallop theorem and the dipolar nature of the far flow field. We discuss the consequences of these to the velocity field of a swimmer suspension and to the motion of passive tracers as a bacterium swims past.

1 Introduction

Swimming at low Reynolds number [1–3], the regime appropriate to microscopic swimmers examples of which are shown in Fig. 1, is a classical problem, addressed by many well-known mathematicians through the 20th century [4–8]. There has been something of a microswimmer renaissance lately, which one might speculate is driven by advances in tracking and microfluidic technologies allowing more quantitative experiments, together with increasing cross-disciplinary initiatives across the physical and biological sciences.

A theoretical understanding of how microswimmers move, and stir the fluid that surrounds them, is helpful in many respects. It is interesting to ask about the links between evolution and swimming strategies: for example are there particular swimming strokes which help a bacterium to move in a viscoelastic environment such as the gut [9]? There are many attempts both to fabricate swimming micro-robots, which could be used for targeted drug delivery, and to harness bacteria themselves to transport payloads or drive nanomachines [10,11,2]. Moreover microswimmers are one of the most accessible examples of active systems [12], entities that produce their own energy and hence operate out of thermodynamic equilibrium, and hence swimmer suspensions provide a testing ground for non-equilibrium statistical physics.

This manuscript is a summary of a set of lectures given at the Geilo School 2013 *Soft Matter Confinement: from Biology to Physics*. It aims to provide an introduction to the hydrodynamics that underlies the way in which microorganisms, such as

[a] e-mail: J.Yeomans1@physics.ox.ac.uk

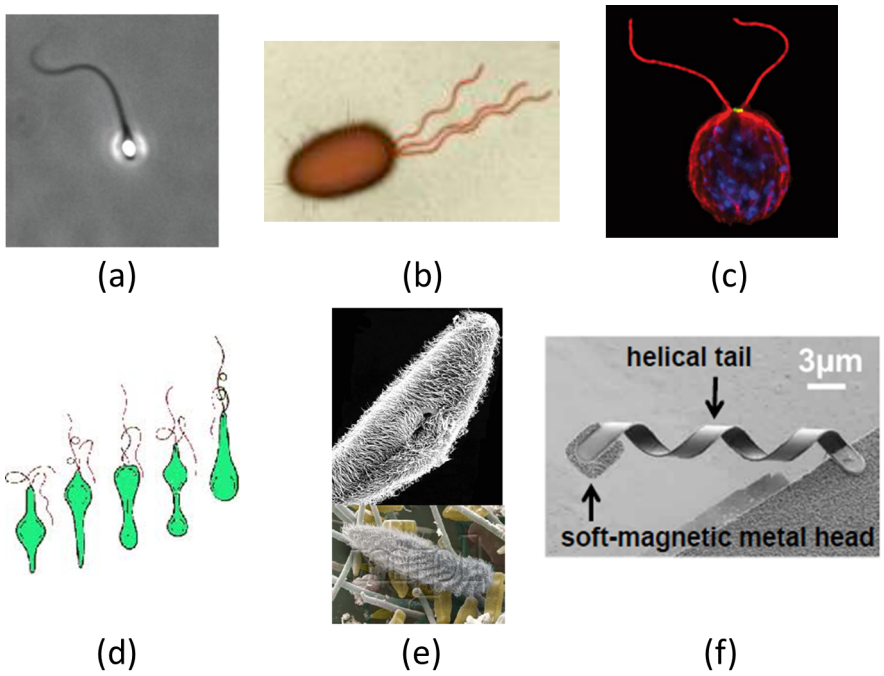

Fig. 1. Low Reynolds number swimmers: (a) a sperm cell [13], the wave moving along the flagellum defines a direction in time and allows motion at zero Reynolds number; (b) *E. coli*, an example of a pusher, the far flow circulates outwards from the head and tail and inwards to the sides; (c) *Chlamydomonas*, the 'breast-stroke' of the flagella leads to a contractile (puller) far flow which circulates from the sides to the front and rear; (d) *Euglena metaboly*, shape changes of the body result in propulsion; (e) *Paramecium*, the surface is covered by beating cilia, these synchronise, and metachronal waves in the beating pattern move across the surface of the organism; (f) a fabricated microswimmer, driven by a rotating magnetic field [11].

bacteria and algae, and fabricated microswimmers, swim. For such tiny entities the governing equations are the Stokes equations, the zero Reynolds number limit of the Navier-Stokes equations. This implies the well-known Scallop Theorem, that swimming strokes must be non-invariant under time reversal to allow a net motion, ideas introduced in Sec. 2. Then, in Sec. 3, we define two model microswimmers and show how to calculate their swimming speeds.

A concept that we stress in this review is that biological swimmers move autonomously, free from any net external force or torque. As a result the leading order term in the multipole (far field) expansion of the Stokes equations vanishes and microswimmers generically have dipolar far flow fields. Sec. 4 is a discussion of the multipole expansion, and its application to microswimming, and we introduce the *stresslet* and *rotlet*. Then, in Sec 5, we describe physical examples where the dipolar nature of the bacterial flow field has significant consequences, velocity statistics in a dilute bacterial suspension and tracer diffusion in a swimmer suspension. A discussion of open questions in Sec. 6 closes the paper. As this is a tutorial review we have aimed to cite references which can be used as entries to the literature.

2 Zero Reynolds number and the Scallop theorem

The Navier-Stokes equations for an incompressible fluid [14] describe the evolution of the velocity $\mathbf{v}(\mathbf{r},t)$ of a fluid of density ρ and dynamic viscosity μ driven by a pressure gradient ∇p and a body force (force per unit volume) $\mathbf{f}$:

$$\rho\left\{\frac{\partial \mathbf{v}}{\partial t}+(\mathbf{v}\cdot\nabla)\mathbf{v}\right\}=-\nabla p+\mu\nabla^2\mathbf{v}+\mathbf{f},\qquad \nabla\cdot\mathbf{v}=0. \tag{1}$$

Dimensionless variables, denoted by a tilde, can be defined by choosing a length scale L_0 and a velocity scale V_0

$$\tilde{v}=\frac{v}{V_0},\qquad \tilde{x}=\frac{x}{L_0},\qquad \tilde{\nabla}=L_0\nabla,\qquad \tilde{t}=\frac{V_0}{L_0}t,\qquad \frac{\partial}{\partial\tilde{t}}=\frac{L_0}{V_0}\frac{\partial}{\partial t}. \tag{2}$$

In terms of the dimensionless variables the Navier-Stokes equation becomes

$$\left\{\frac{\partial\tilde{\mathbf{v}}}{\partial\tilde{t}}+(\tilde{\mathbf{v}}\cdot\tilde{\nabla})\tilde{\mathbf{v}}\right\}=-\frac{L_0}{V_0^2\rho}\nabla p+\frac{\mu}{L_0V_0\rho}\tilde{\nabla}^2\tilde{\mathbf{v}}+\frac{L_0}{V_0^2\rho}\mathbf{f}. \tag{3}$$

The terms on the left hand side of this equation are the inertial terms. They describe the flow of momentum through the fluid, and are a direct consequence of momentum conservation. The second term on the right-hand side is the viscous term. This describes the dissipation that relaxes any velocity gradients. The balance of inertial and viscous contributions to a fluid's flow is described by the dimensionless Reynolds number, which follows immediately from the coefficient of the viscous term in Eq. (3)

$$\mathrm{Re}=\frac{\text{inertial response}}{\text{viscous response}}\sim\frac{\rho L_0V_0}{\mu}. \tag{4}$$

For microswimmers typical sizes and velocities are 10^{-5}m and 10^{-5}ms^{-1} giving Re$\sim 10^{-4}$ for swimming in water. Hence the zero Reynolds number limit is normally used to describe microswimming. This appears to work well: indeed Lauga [15] has pointed out that Re=0 is not a singular limit so small values should not qualitatively affect swimmer behaviour. However, the unsteady (time-derivative) term in Eq. (1) or multiple swimmer configurations, when the appropriate length scale is the distance between swimmers rather than the swimmer size, could lead to inertial corrections.

At zero Reynolds number the Navier-Stokes equations reduce to the Stokes equations

$$\nabla p=\mu\nabla^2\mathbf{v}+\mathbf{f},\qquad \nabla\cdot\mathbf{v}=0. \tag{5}$$

The presence of a swimmer in the fluid is embodied in $\mathbf{f}$: as the swimmer moves it exerts forces on the fluid setting up a flow field.

A fundamental consequence of the Stokes limit is the Scallop Theorem [16,17]. This states that a swimmer must have a swimming stroke that is not invariant under time reversal if it is to move. This is a consequence of the lack of time dependence in the Stokes Eqs. (5). There is nothing in the equations themselves that can lead to an asymmetry in time. Therefore the source of the flow, the swimming stroke, must break time-reversal symmetry for there to be a preferred direction of motion. A zero Reynolds number swimmer with a stroke that looks the same forward and backwards in time may oscillate and create a flow field, but the net displacement over a stroke will average to zero.

A glance at the microorganisms in Fig. 1 shows how they have evolved to beat the Scallop Theorem. The wave moving down the flagella of *Escherichia coli* or sperm defines a direction in time. *Paramecium* is covered by cilia, similar to those that

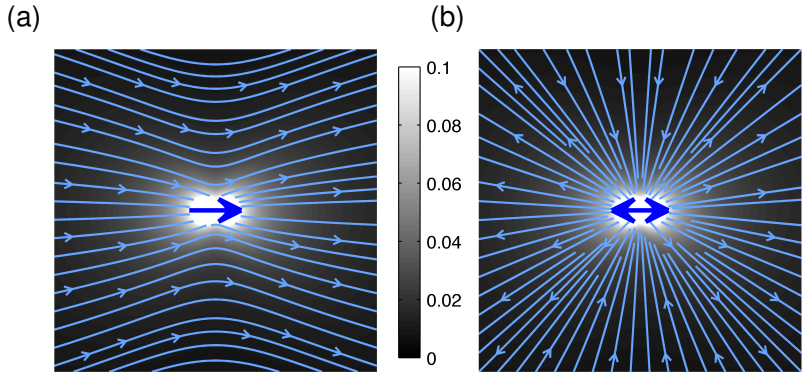

Fig. 2. Far flow fields produced by (a) a Stokeslet (colloid) (b) a stresslet (microswimmer). Note the very different symmetries.

clear mucus from the lungs, that have distinct power and recovery strokes. *Euglena metaboly* produces a suitable swimming stroke by altering its body shape.

For a point force acting at the origin the Stokes equations (5) can be solved exactly. The resulting velocity field, termed the Stokeslet, and the corresponding pressure field, at a relative position $\mathbf{r}$ from the swimmer are

$$\mathbf{v} = \frac{\mathbf{f}}{8\pi\mu} \cdot \left(\frac{\mathbf{I}}{r} + \frac{\mathbf{rr}}{r^3} \right) \equiv \mathbf{G} \cdot \mathbf{f}, \qquad p = p_0 + \frac{\mathbf{f} \cdot \mathbf{r}}{4\pi r^3}. \tag{6}$$

In (6) $\mathbf{I}$ is the unit tensor, and p_0 is a reference, constant pressure. $\mathbf{G}$ is the Green's function of the Stokes equations, often called the Oseen tensor (and often defined having removed the factor $\frac{1}{8\pi\mu}$). There are several ways of obtaining the Stokeslet, none of them very simple. A clear and helpful list of the possible approaches is given by Maciej Lisicki at http://www.fuw.edu.pl/~mklis/publications/Hydro/oseen.pdf.

To give a physical interpretation of the Stokeslet we write down the velocity field created by a colloid of radius a moving through a fluid with velocity $\mathbf{u}$ with non-slip boundary conditions. This is an exact expression for a spherical particle, lengthy to derive [14], but easily checked by substituting in Eqs. (5),

$$\mathbf{v}_{\text{sphere}} = \frac{\mathbf{u}}{r} \left(\frac{3a}{4} + \frac{a^3}{4r^2} \right) + \frac{(\mathbf{u} \cdot \mathbf{r})\mathbf{r}}{r^2} \left(\frac{3a}{4r} - \frac{3a^3}{4r^3} \right). \tag{7}$$

In the limit of a point colloid $a \ll r$ (or equivalently sufficiently far from a colloid of finite radius) this expression reduces to the Stokeslet if

$$\mathbf{f} = 6\pi\mu a \mathbf{u} \tag{8}$$

the familiar expression for Stokes drag, the force needed to pull a colloid through a fluid with velocity $\mathbf{u}$. The velocity field produced by a colloid is shown in Fig. 2(a). Note that it decays with distance as r^{-1}. We shall highlight a different dependence for bacteria.

3 Model swimmers

Minimal models, designed to circumvent the restrictions of the Scallop Theorem, are a useful tool to help understand the hydrodynamics of microswimming [18–20]. Here

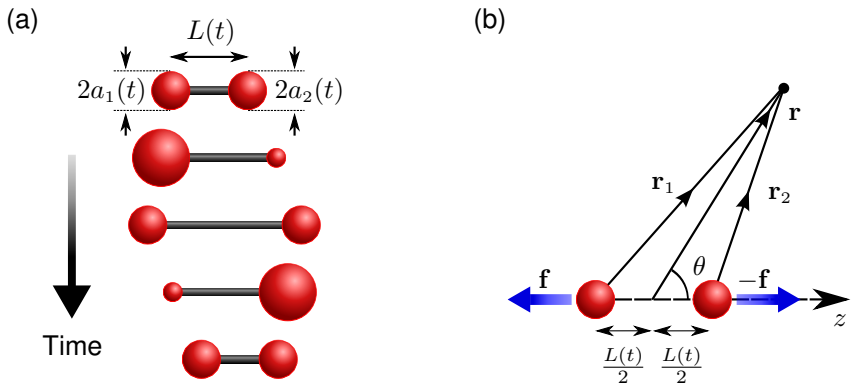

Fig. 3. (a) The swimming stroke of Vic's swimmer. (b) Geometry used in the calculation of the dipole flow field.

we introduce two, of many, model swimmers. The first, nicknamed 'Vic's swimmer', is an example of the genre of models made up of a collection of small, linked spheres whose relative motion defines the swimming stroke. These are useful because the flow field set up by a forced sphere is known in the Stokes limit and, because the Stokes equations are linear, the swimmer velocity field can be obtained by summing the contributions from each individual sphere. The second system, squirmers, included by way of contrast, has proved particularly appropriate for numerical work [21].

3.1 Vic's swimmer

Vic's swimmer was defined by Lt.Col. Victor B. Putz (U.S. Air Force) during his time as a graduate student at Oxford [22,23]. It builds on earlier work by Avron *et al.* [19] and bears a passing resemblance to *E. metaboly*, pictured in Fig. 1. Vic's swimmer consists of two small spheres, joined by a thin, rigid rod, see Fig. 3. The radii of sphere $i = 1, 2$ change with time as $a_i(t) = a + \lambda \sin(\omega t + \varphi_i)$ and the length of the rod oscillates as $L(t) = l + \xi \sin(\omega t + \alpha)$. Here our aim is to use the model as a simple example of how to calculate the swimming speed of linked-sphere swimmers. We shall also, in Section 4, give an expression for the far flow field of Vic's swimmer.

To drive the motion a force $\mathbf{f}_i(t)$ must act on each sphere. These are internal forces - **no net force acts on the swimmer which is internally driven** - and hence $\mathbf{f}_1 = -\mathbf{f}_2 \equiv \mathbf{f}$. Assuming the spheres move along the z-axis, and that their radii are always small compared to their separation, we may write expressions for the velocity of each sphere

$$\dot{z}_1 = \frac{f_1}{6\pi\mu a_1} + \frac{f_2}{4\pi\mu L} = +\frac{f}{6\pi\mu a_1} - \frac{f}{4\pi\mu L}, \tag{9}$$

$$\dot{z}_2 = \frac{f_2}{6\pi\mu a_2} + \frac{f_1}{4\pi\mu L} = -\frac{f}{6\pi\mu a_2} + \frac{f}{4\pi\mu L}. \tag{10}$$

The first term in each expression is the Stokes drag on the sphere Eq. (8); the second is the contribution to the velocity field from the other sphere, assumed to act as a Stokeslet, given by Eq. (6). The constraint that the rod is rigid serves to close the

equations

$$L(t) = z_2 - z_1, \qquad \dot{L}(t) = \dot{z}_2 - \dot{z}_1 \tag{11}$$

which can be solved for $\dot{z}_1$, $\dot{z}_2$ and $\mathbf{f}$.

The velocity of the midpoint of the swimmer is

$$\frac{d\bar{z}}{dt} := \frac{\dot{z}_1 + \dot{z}_2}{2} = \frac{(\dot{z}_1 - \dot{z}_2)}{12\pi\mu}\left(\frac{1}{a_1} - \frac{1}{a_2}\right)\left\{\frac{1}{6\pi\mu}\left(\frac{1}{a_1} + \frac{1}{a_2}\right) - \frac{2}{4\pi\mu L}\right\}^{-1}. \tag{12}$$

For $a_1 \approx a_2 \ll L$, and substituting in the time dependence of these variables:

$$\frac{d\bar{z}}{dt} \approx \frac{\lambda\omega\xi\cos(\omega t + \alpha)}{4a}\{\sin(\omega t + \varphi_2) - \sin(\omega t + \varphi_1)\}. \tag{13}$$

This leads to a time-averaged swimmer velocity

$$u_{\text{swimmer}} = \frac{\lambda\omega\xi}{4a}\sin\Delta\varphi\cos\Delta\alpha \tag{14}$$

where

$$\Delta\varphi = \frac{(\varphi_1 - \varphi_2)}{2}, \qquad \Delta\alpha = \frac{(\varphi_1 + \varphi_2)}{2} - \alpha. \tag{15}$$

The average swimmer velocity is zero for $\Delta\varphi = 0, \pi$. This is because, if the drag of the spheres changes in phase, the stroke is time reversible and there is no movement because of the Scallop Theorem. u_{swimmer} is also zero for $\Delta\alpha = \pi/2, 3\pi/2$. These zeros are not based on a symmetry principle, and they will disappear at higher order. Note also that, in the interests of simplicity, we have ignored any flow induced by the swimmer as the sphere radii change.

3.2 Squirmers

Squirmers [20,24] represent a different class of model swimmers, useful because they admit an exact solution and also because they are spherical which helps to disentangle steric and hydrodynamic effects. Motion arises by imposing suitable velocity boundary conditions on a spherical surface of radius a. Defining a spherical polar coordinate system with the squirmer velocity along z we assume a zero radial velocity at the surface, and write the tangential surface velocity as a power series in the first derivatives of the Legendre polynomials

$$v_\theta(a,\theta) = \sum_{n=1}^{\infty} B_n \frac{2}{n(n+1)}\sin\theta P_n'(\cos\theta) \tag{16}$$

where the B_n can depend on time. It is easy to check that the solution to the Stokes equation which obeys these boundary conditions is

$$\begin{aligned} v_r(r,\theta) &= \frac{2}{3}B_1\cos\theta + \frac{2B_1}{3}\frac{a^3}{r^3}P_1 + \sum_{n=2}^{\infty}\left(\frac{a^{n+2}}{r^{n+2}} - \frac{a^n}{r^n}\right)B_n P_n, \\ v_\theta(r,\theta) &= -\frac{2}{3}B_1\sin\theta + \frac{B_1}{3}\frac{a^3}{r^3}\sin\theta P_1' + \sum_{n=2}^{\infty}\left(\frac{1}{(n+1)}\frac{a^{n+2}}{r^{n+2}} - \frac{(n-2)}{n(n+1)}\frac{a^n}{r^n}\right)\sin\theta B_n P_n' \end{aligned} \tag{17}$$

in the rest frame of the squirmer, which is moving with velocity $\frac{2}{3}B_1$ along the z-axis.

For the simplest non-trivial example, $B_n = 0, \quad n > 2$, and recalling that $P_1 = \cos\theta$ and $P_2 = (3\cos^2\theta - 1)/2$ the velocity field reduces to

$$v_r(r,\theta) = \frac{2}{3}B_1\cos\theta + \frac{2B_1}{3}\frac{a^3}{r^3}\cos\theta - \frac{a^2}{r^2}\frac{B_2}{2}(3\cos^2\theta - 1) + O\left(\frac{a^4}{r^4}\right),$$
$$v_\theta(r,\theta) = -\frac{2}{3}B_1\sin\theta + \frac{B_1}{3}\frac{a^3}{r^3}\sin\theta + O\left(\frac{a^4}{r^4}\right). \tag{18}$$

Recent work has considered interactions between squirmers [21], and experiments on self-propelled colloids have been interpreted in terms of a squirmer model [25]. There have also been several recent numerical studies of the hydrodynamics of many squirmers [26]. Clustering has been observed as the squirmer concentration increases, but details of this appear to depend sensitively on steric interactions and the parameters of the model, and there is no clear understanding of the multi-squirmer dynamics as yet.

4 Far flow field

We next calculate the far flow field produced by a swimmer. Just as in the case of the electrostatic potential which solves the Laplace equation, the Stokes equation has a multipole expansion, where the velocity field can be written as a power series in r^{-1}, where r is the distance from the swimmer. We have shown in Sec. 2 that the flow field due to a driven colloid $\sim r^{-1}$ at large r. We shall now argue that, generically, the far field velocity of a swimmer is *dipolar*, decaying as r^{-2}.

This is because biological microswimmers produce their own driving. There is no net external force or torque, assuming the organism is neutrally bouyant. All internal forces and torques, that result in the motion must balance giving a cancellation of the leading r^{-1} term in the multipole expansion. The analogous situation in electrostatics is the electric dipole, closely spaced, balanced, positive and negative charges that produce a dipolar electric field. We illustrate this for a pair of balanced forces, and then give a more general development of the multipole expansion.

4.1 Balanced forces and the dipolar field

Consider a pair of equal and opposite point forces, $\mathbf{f}$, acting co-linearly in a Stokes fluid. (This is the situation shown for Vic's swimmer in Fig. 3, sufficiently far from the swimmer that the finite sphere radius can be neglected.) The velocity field due to the two Stokeslets is

$$\mathbf{v}(\mathbf{r}) = \frac{\mathbf{f}}{8\pi\mu}\cdot\left(\frac{\mathbf{I}}{r_1} + \frac{\mathbf{r_1}\mathbf{r_1}}{r_1^3}\right) - \frac{\mathbf{f}}{8\pi\mu}\cdot\left(\frac{\mathbf{I}}{r_2} + \frac{\mathbf{r_2}\mathbf{r_2}}{r_2^3}\right) \tag{19}$$

where $\mathbf{r}_i$ is the distance from the i^{th} Stokeslet to the point of observation $\mathbf{r}$. Using the polar co-ordinate system shown in Fig. 3(b), with the forces acting along z, and the Stokeslets separated by a distance $\ell \ll r$ expanding this expression gives

$$\mathbf{v} = \frac{f}{8\pi\mu}\ \frac{\ell}{r^2}\ (3\cos^2\theta - 1)\hat{\mathbf{r}}. \tag{20}$$

Note the signature r^{-2} dipolar decay. The angular dependence of the flow field is shown in Fig. 2(b). Contrasting it to the colloidal field in Fig. 2(a) there is reflection

symmetry about the plane perpendicular to the swimmer. This will be relevant when we consider the movement of tracers in a swimmer suspension in Sec. 5 below. The figure is drawn for $f > 0$ where the fluid is pushed away from the ends of the swimmer along the direction of motion. This is termed an extensile swimmer or pusher. For $f < 0$ the direction of the velocity field is reversed giving a contractile swimmer or puller. *E. coli* and *Chlamydomonas reinhardtii* are examples of pushers and pullers, respectively.

4.2 Multipole expansion

We now obtain a general expression for the dipolar, and higher order, contributions to a Stokesian flow field showing in particular that the dipole moment is, in general, a second rank, traceless tensor and the quadrupole moment a third rank tensor. We then indicate how the results reduce to the simpler expression (20) [27,28].

We extend Eq. (6) to a force distribution $\mathbf{f}(\xi)$

$$v_i(\mathbf{r}) = \int G_{ij}(\mathbf{r}-\xi) f_j(\xi)\, d\xi \tag{21}$$

where

$$G_{ij}(\mathbf{r}-\xi) = \frac{1}{8\pi\mu}\left(\frac{\delta_{ij}}{\mid \mathbf{r}-\xi \mid} + \frac{(\mathbf{r}-\xi)_i(\mathbf{r}-\xi)_j}{\mid \mathbf{r}-\xi \mid^3}\right). \tag{22}$$

Taylor expanding about the origin

$$\begin{aligned} v_i(\mathbf{r}) &= \int \left\{ G_{ij}(\mathbf{r}) - \frac{\partial G_{ij}}{\partial \xi_k}(\mathbf{r})\xi_k + \frac{1}{2}\frac{\partial^2 G_{ij}}{\partial \xi_k \partial \xi_l}(\mathbf{r})\xi_k\xi_l \ldots \right\} f_j(\xi)\, d\xi \\ &= G_{ij}(\mathbf{r}) \int f_j(\xi)\, d\xi - \frac{\partial G_{ij}}{\partial \xi_k}(\mathbf{r}) \int \xi_k f_j(\xi)\, d\xi \\ &\quad + \frac{1}{2}\frac{\partial^2 G_{ij}}{\partial \xi_k \partial \xi_l}(\mathbf{r}) \int \xi_k\xi_l f_j(\xi)\, d\xi + \ldots \\ &\equiv G_{ij}(\mathbf{r})F_j + \frac{\partial G_{ij}}{\partial \xi_k}(\mathbf{r})D_{jk} + \frac{1}{2}\frac{\partial^2 G_{ij}}{\partial \xi_k \partial \xi_l}(\mathbf{r})Q_{jkl} + \ldots \end{aligned} \tag{23}$$

The monopole contribution to the flow field, $G_{ij}(\mathbf{r})F_j$, absent for force-free swimmers, is just the Stokeslet, Eq. (6).

The dipolar tensor is

$$D_{jk} = -\int \xi_k f_j\, d\xi. \tag{24}$$

It is conventional to write

$$D_{jk} - \frac{1}{3}D_{ii}\delta_{jk} = S_{jk} + T_{jk} \tag{25}$$

where S_{jk} is a traceless symmetric tensor, referred to as the *stresslet*, and T_{jk} is an asymmetric tensor, the *rotlet*. Subtracting $\frac{1}{3}D_{ii}\delta_{jk}$ is permissible because $\nabla \cdot \mathbf{G} = 0$ and hence this term does not change the velocity field.

The stresslet

$$S_{jk} = -\frac{1}{2}\int (\xi_k f_j + \xi_j f_k)\, d\xi + \frac{1}{3}\int \xi_i f_i\, \delta_{jk}\, d\xi \tag{26}$$

is connected to straining flows, and is responsible for the changes in viscosity of a fluid in the presence of colloids or swimmers. In the frame where the S_{jk} is diagonal

there will, in general, be two independent dipole moments contributing to the flow field.

As a concrete example, and to check that we recover the dipolar flow field given in Eq. (20), we consider a force distribution that is axisymmetric about, say, the z-axis:

$$\mathbf{f} = f_z(\rho, z)\mathbf{e}_z + f_\rho(\rho, z)\mathbf{e}_\rho + f_\varphi(\rho, z)\mathbf{e}_\varphi \tag{27}$$

where we use standard cylindrical polar co-ordinates (ρ, φ, z), and $\{\mathbf{e}\}$ are the associated unit vectors. Then recalling that

$$\begin{aligned} f_x &= f_\rho \cos\varphi - f_\varphi \sin\varphi, \\ f_y &= f_\rho \sin\varphi + f_\varphi \cos\varphi \end{aligned} \tag{28}$$

it is straightforward to show that

$$S_{zz} = \int (\rho f_\rho - 2z f_z)/3 \; d\xi, \tag{29}$$

$$S_{xx} = S_{yy} = -S_{zz}/2 \tag{30}$$

with all the off diagonal terms zero by symmetry.

The corresponding contribution to the velocity field is

$$\frac{\partial G_{ij}}{\partial \xi_k}(\mathbf{r}) S_{jk} \tag{31}$$

Recalling the summation over repeated indices, and using the relation between the diagonal components of $\mathbf{S}$, Eq. (30), and the derivatives of $G_{ij}(\mathbf{r})$,

$$\frac{\partial G_{ij}}{\partial \xi_k}(\mathbf{r}) = \frac{1}{8\pi\mu}\left\{-\frac{1}{r^3}\delta_{ij}\xi_k + \frac{1}{r^3}(\delta_{ik}\xi_j + \delta_{jk}\xi_i) - \frac{3}{r^5}\xi_i\xi_j\xi_k\right\}, \tag{32}$$

gives

$$v_i = \frac{1}{8\pi\mu}\frac{3\xi_i}{2r^5}(r^2 - 3z^2)S_{zz} \tag{33}$$

corresponding to a resultant velocity field in the radial direction

$$v_r = \frac{1}{8\pi\mu}\frac{3}{2r^2}(1 - 3\cos^2\theta)S_{zz}. \tag{34}$$

For a swimmer, with point forces of strength f along the z-axis $z = \pm\ell/2$,

$$S_{zz} = -\frac{2}{3}\ell f \tag{35}$$

and hence we recover Eq. (20) for the flow field due to a pair of equal and opposite forces acting along the polar axis.

The rotlet

$$T_{jk} = -\frac{1}{2}\int (\xi_k f_j - \xi_j f_k) \; d\xi \tag{36}$$

can be interpreted physically by noting that the torque $\mathbf{\Gamma}$ exerted by a force distribution on the surrounding fluid is

$$\Gamma_i = -\epsilon_{ijk}\int f_j \xi_k \; d\xi \equiv \epsilon_{ijk} T_{jk}. \tag{37}$$

The asymmetry of T combined with the properties of ϵ_{ijk} mean that this expression can be inverted to give

$$T_{jk} = \frac{1}{2}\epsilon_{jkl}\Gamma_l. \tag{38}$$

The corresponding term in the multipole expansion (23) is

$$\frac{\partial G_{ij}}{\partial \xi_k}(\mathbf{r})T_{jk} = \frac{1}{2}\epsilon_{jkl}\Gamma_l\frac{\partial G_{ij}}{\partial \xi_k} = -\frac{1}{2}(\mathbf{\Gamma}\times\nabla)_j G_{ij} = -\frac{1}{2}\mathbf{\Gamma}\cdot(\nabla\times\mathbf{G}). \tag{39}$$

For the special case of uniaxial symmetry

$$\begin{aligned} T_{xy} = -T_{yx} &= \frac{1}{2}\int \rho f_\varphi \, d\xi, \\ \Gamma_z &= \int \rho f_\varphi \, d\xi, \end{aligned} \tag{40}$$

as expected from the definition of torque, with all other components zero. The corresponding flow field has components

$$\begin{aligned} v_x &= \frac{1}{8\pi\mu}\left\{-\frac{2y}{r^3}\right\}T_{xy}, \\ v_y &= \frac{1}{8\pi\mu}\left\{+\frac{2x}{r^3}\right\}T_{xy}, \\ v_z &= 0 \end{aligned} \tag{41}$$

equivalent to a velocity

$$v_\varphi = \frac{1}{8\pi\mu}\frac{2}{r^2}T_{xy}. \tag{42}$$

The rotlet was included for completeness, but self-propelled swimmers and bacteria are torque free so this term does not appear in the multipole expansion. At higher order, the counter-rotating head and tail of, for example, *E. coli* produce a rotlet dipole, one consequence of which is that they swim in circular trajectories near a surface.

4.3 Far flow field of the model swimmers

Vic's swimmer: For Vic's swimmer, solving Eqs. (9)–(11) for the force, substituting into Eq. (20), and averaging over time, the far flow field is

$$v_{\text{swimmer}} = \frac{1}{4\pi\mu}\frac{3\lambda\omega\xi l}{16}\cos\Delta\varphi\sin\Delta\alpha\frac{(3\cos^2\theta-1)}{r^2} \tag{43}$$

where $\Delta\varphi$ and $\Delta\alpha$ are defined by Eq. (15). The dipolar contribution to the flow field disappears for $\Delta\alpha = 0, \pi$. For these values the swimmer is invariant under time reversal, followed by a parity transformation $\mathbf{r}\to-\mathbf{r}$, and the leading term is quadrupolar, $\sim r^{-3}$. Comparing Eqs. (14) for the velocity of the swimmer and (43) for the far flow field it is apparent that a fast swimmer does not necessarily produce a strong far field velocity; the swimming speed is set by the near field.

Squirmer: Reading from Eq. (17) the squirmer has a dipole moment $(8\pi\mu)B_2a^2/3$. Note that for this model the velocity and quadrupole moment $\sim(8\pi\mu)B_1a^3$ are not independent.

5 Consequences of the dipolar flow field

We have argued that, because no external force or torque acts on the swimmer, it has a dipolar (or higher order) far flow field. This has several consequences, which lead to significant differences between the hydrodynamic properties of a suspension of swimmers and, say, a suspension of driven colloids. We give three examples:

5.1 Velocity distribution of a dilute swimmer suspension

We consider the probability distribution function of the velocity at a point, the origin say, in a suspension of non-interacting swimmers [29]. The magnitude of the velocity due to a single swimmer scales as $v \sim r^{-n}$ where $n = 3$ for a quadrupolar swimmer, $n = 2$ for a dipolar swimmer, and $n = 1$ for a driven swimmer or colloid. Assuming that the swimmers are non-interacting and distributed isotropically in space

$$P(r)dr \sim r^2 dr, \qquad P(v)dv \sim v^{-(1-3/n)}dv. \tag{44}$$

The probability distribution function for the velocity at a point due to a single swimmer is a power law. For many swimmers the linearity of the Stokes equations means that the contributions from each swimmer can be summed, and the first surmise would be that the Central Limit Theorem predicts a rapid crossover to a Gaussian distribution of the velocity. However, the Central Limit Theorem only holds for a distribution function with a finite variance and, because of the divergence of $P(v)$ at small distances, its variance is finite only for $n < 3/2$. Hence for $n > 3/2$ power law tails persist in the distribution for all swimmer concentrations. This argument must be supplemented by noting that in a physical system the short distance divergence of the velocity will be truncated, by higher order terms in the multipole expansion, and by the finite size of the swimmers. Hence there will be a slow crossover to Gaussian behaviour but with marked power law tails persisting to high concentrations.

Indirect evidence for this behaviour has been observed by Leptos *et al.* [30], who measured the probability distribution function of the displacement of tracer particles in a dilute suspension of *Chlamydomonas* as a function of the concentration of the swimmers. The data was taken after 1s, a time over which it is reasonable to approximate displacement as proportional to a constant velocity, and therefore to assume that the displacement and velocity distributions are similar. Pronounced tails are seen in the data, corresponding to close approaches of swimmers and tracer particles. This should be compared to similar experiments on *Volvox*, a swimmer which is sufficiently large that the force of gravity is appreciable [31]. Hence the far flow field of *Volvox* has a leading order term $\sim r^{-1}$ leading to a much quicker crossover to Gaussian behaviour and less prominent tails in the displacement distribution.

5.2 Tracer loops

Next we discuss the diffusion constant of tracer particles in a bacterial suspension [32, 33]. Several experiments and simulations have shown that bacteria enhance diffusion as a result of the flow fields they produce [30,34,35], and it is likely that this has the advantage of helping to increase their nutrient supply. One might also image 'stealth swimmers', anxious to avoid detection, that move in such a way as to to minimise any far field flows. To fully understand the link between function and swimming stroke we need to unravel how microswimmers act as stirrers.

The instantaneous statistics of the velocity field govern the initial rate of displacement of a tracer particle. However at later times the path taken by a tracer

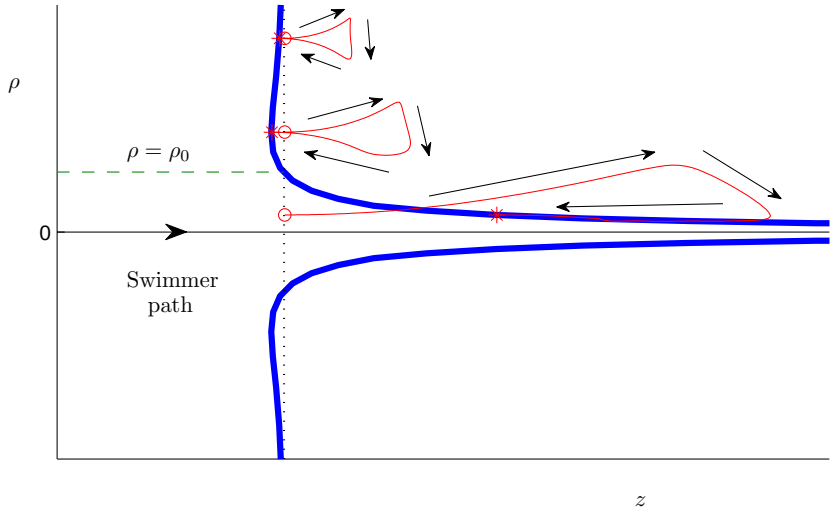

Fig. 4. Typical motion of a sheet of tracer particles as a swimmer moves in an infinite straight trajectory from $z = -\infty$ to $z = +\infty$ perpendicular to the sheet. The initial position of the tracer sheet is shown as a dotted line, and the envelope of the final tracer positions in blue. Examples of the loop like trajectories of the tracers are indicated as lighter, red lines.

will depend on the detailed spatial and temporal correlations of the velocity. The symmetry of the velocity field corresponding to multipoles with $n > 1$ means that tracers move in a quantitatively different way as a force-free swimmer (stresslet) or as a colloid (Stokeslet) move past.

Consider a swimmer that moves in a straight line from $-\infty$ to $+\infty$ along the z-axis. The resulting displacement of a material sheet, a plane of tracers initially perpendicular to the swimmer path is shown in Fig. 5.1. Tracers far from the swimmer are pushed backwards, those close to the swimmer pulled forwards. The tracers move in loops, a consequence of the symmetry of these flow fields [23]. If the tracer is sufficiently far from the swimmer that its velocity can be neglected compared to the swimmer velocity the loops are closed. The closed nature of the loops can be inferred from the geometry of the flow field, but a simple mathematical proof helps to pinpoint the approximations under which the loops are indeed fully closed [33].

In the absence of the Stokeslet it follows from Eq. (23) that the flow field produced by the swimmer takes the form

$$\mathbf{u}\left(\mathbf{r},\mathbf{k}\right) = \left(\mathbf{e_z}\cdot\nabla\right)\mathbf{U}_0\left(\mathbf{r},\mathbf{k}\right) \equiv \frac{d\mathbf{r}_T}{dt} \tag{45}$$

where $\mathbf{r}_T$ is the position of the tracer and $\mathbf{U}_0$ is a velocity field whose Lagrangian derivative at the position of the tracer $\mathbf{r}_T$ is

$$\frac{d\mathbf{U}_0}{dt} = \left(\mathbf{V}\cdot\nabla\right)\mathbf{U}_0 - \left(\frac{d\mathbf{r}_T}{dt}\cdot\nabla\right)\mathbf{U}_0. \tag{46}$$

Taking the swimmer velocity $\mathbf{V} = V\mathbf{e_z}$ and keeping just the Eulerian term

$$\frac{d\mathbf{U}_0}{dt} \approx V\left(\mathbf{e_z}\cdot\nabla\right)\mathbf{U}_0. \tag{47}$$

Comparing Eqs. (45) and (47) gives a tracer velocity

$$\frac{d\mathbf{r}_T}{dt} \approx \frac{1}{V}\frac{d\mathbf{U}_0}{dt} \tag{48}$$

and a total tracer displacement for the infinite, linear swimmer path

$$\Delta\mathbf{r}_T = \int_{-\infty}^{+\infty} \frac{d\mathbf{r}_T}{dt} dt = -\frac{\kappa}{V}\left(\mathbf{U}_0(+\infty) - \mathbf{U}_0(-\infty)\right) = \mathbf{0}. \tag{49}$$

Enhanced diffusion of the tracers in a swimmer suspension could not occur if the tracers simply moved in closed loops, and mechanisms for non-closure can usefully be identified from the approximations inherent in this proof. Firstly, the Lagrangian contribution to the time derivative of the tracer velocity, which arises because the tracer moves across stream lines was neglected in Eq. (47). This becomes increasingly important as the tracer is closer to the swimmer and hence moves faster. At short distances, the tracer is entrained by the swimmer (see Fig. 5.1).

Perhaps surprisingly, the total volume of fluid displaced by the swimmer as it moves along an infinite, straight path takes a simple, universal form [36,37,33]

$$v_D = \frac{4\pi Q_\perp}{V} - v_s - v_{\text{wake}} \tag{50}$$

where v_s and v_{wake} are the volumes of the swimmer and its wake and $Q_\perp = -\frac{1}{2}\int f_z \rho^2 \, dS$ is a quadrupole moment. v_D is termed the Darwin drift: by comparison, for a colloid at zero Reynolds number this quantity is infinite.

Secondly it is apparent from Eq. (49) that a finite swimmer path length will lead to loops that are not closed. Bacteria do not move along infinite straight paths because of rotational diffusion. Indeed some microorganisms, for example *E. coli* have an explicit run and tumble behaviour which allows them to exploit a directed random walk to move up a nutrient gradient. This important contribution to tracer diffusion is an ongoing area of research. Another open question is the importance of dimensionality: experimental work has shown a substantial increase of diffusivity in thin films [38].

6 Discussion

In these notes we have concentrated on individual swimmers in a simple fluid emphasising two features which characterise swimming at zero Reynolds number. The first of these is the Scallop Theorem which demands that the stroke of a microswimmer is non-invariant under time reversal. The second is the dipolar nature of the far flow field of microswimmers which results from their motion being autonomous, and hence force and torque free. We have shown that these properties lead to swimming strokes and flow fields very different to those relevant on human length scales. In conclusion we briefly summarise some questions of current interest: for a recent special journal issue on *Active Matter* see [39] .

One example is the effects of surfaces and interfaces on microscopic swimming: many experiments are most easily performed in confined geometries and certain microorganisms, such as sperm, are strongly attracted to surfaces. Hydrodynamic behaviour is altered by the presence of a no-slip wall, with the Oseen tensor being replaced by the Blake tensor [7], and there is current discussion about whether hydrodynamic or steric forces are dominant in controlling swimming trajectories near surfaces [40,41].

Bacteria survive in an incredible range of places, many in viscoelastic fluids such as mucus, and in highly crowded environments [42, 43]. There is a lot to understand about swimming strategies in the presence of polymers, colloids and biomolecules, which may be much smaller than, but could also be of similar size to, the microswimmers themselves. One might speculate about evolutionary strategies that have matched bacterial shape and stroke to their host fluid.

We have concentrated primarily on theoretical aspects of low Reynolds number hydrodynamics, but calculations are often inspired by experiments using enhanced particle tracking techniques to follow the motion of single or multiple microorganisms and to characterise the surrounding flow fields. Moreover, many groups are working to fabricate microswimmers, from self-propelled colloids, which can be driven by chemical gradients or activated by light, to the magnetically-driven helical ribbons, shown in Fig. 1(f). Potential applications include mixing or transport in microchannels, and as machines transforming chemical energy to mechanical work.

Finally, denser microswimmer suspensions provide examples of collective systems that are operating out of thermodynamic equilibrium. In common with other active systems, such as active colloids, molecular motors, shoals of fish and vibrated granular matter, swimmers show transient clustering and, at higher densities, 'turbulent'-like flow patterns [12]. Formulating a non-equilibrium statistical physics to describe active matter is an exciting and topical avenue for research.

Acknowledgments: We thank J. Dunkel, R. Golestanian, R. Ledesma-Aguilar and V.B. Putz for helpful discussions. JMY and DOP acknowledge funding from the ERC Advanced Grant MiCE.

References

1. E. Lauga and T.R. Powers, Reports on Progress in Physics **72** (2009) 096601
2. S.J. Ebbens and J.R. Howse, Soft Matter **6** (2010) 726
3. J.S. Guasto, R. Rusconi and R. Stocker, Annual Reviews of Fluid Mechanics **44** (2011) 637
4. J. Lighthill, *Mathematical Biofluiddynamics* (Society for Industrial and Applied Mathematics 1975)
5. G.J. Hancock, Proc. Royal Soc. London Series A **217** (1953) 96
6. J.J.L. Higdon, J. Fluid Mech. **90** (1979) 685
7. J.R. Blake, Proc. of the Cambridge Philosophical Society **70** (1971) 303
8. G.K. Batchelor, J. Fluid Mech. **44** (1970) 419
9. J. Teran, L. Fauci and M. Shelley, Phys. Rev. Lett. **104** (2010) 36
10. R. Dreyfus, J. Baudry, M.L. Roper, M. Fermigier, H.A. Stone and J. Bibette, Nature **437** (2005) 862
11. L. Zhang, J.J. Abbott, L.X. Dong, B.E. Kratochvil, D. Bell and B.J. Nelson, Applied Phys. Lett. **94** (2009) 064107
12. M.C. Marchetti, J.F. Joanny, S. Ramaswamy, T.B. Liverpool, J. Prost, M. Rao and R.A. Simha, Rev. Mod. Phys. **85** (2013) 1143
13. E.A. Gaffney, and H. Gadêlha, and D.J. Smith, and J.R. Blake, and J.C. Kirkman-Brown, Ann. Rev. Fluid Mech. **43** (2011) 501
14. L.D. Landau and E.M. Lifshitz, *Fluid mechanics, Course of Theoretical Physics, Vol. 6* (Butterworth-Heinemann 2000)
15. E. Lauga, Soft Matter **7** (2011) 3060
16. E.M. Purcell, American J. of Phys. **20** (1977) 193
17. A. Shapere and F. Wilczek, J. Fluid Mech. **198** (1989) 557
18. A. Najafi and R. Golestanian, Phys. Rev. E **69** (2004) 062901
19. J.E. Avron, O. Kenneth and D.H. Oaknin, New Journal of Physics **7** (1988) 1329

20. M.J. Lighthill, Commun. Pure Appl. Maths **5** 109 (1952)
21. T. Ishikawa, M.P. Simmonds and T.J. Pedley, J Fluid Mech. **568** (2006) 119
22. V.B. Putz, *D. Phil. Thesis: Collective behaviour of model microswimmers* (University of Oxford, 2010)
23. J. Dunkel, V.B. Putz, I.M. Zaid and J.M. Yeomans, Soft Matter **6** (2010) 4268
24. J.R. Blake, J. Fluid Mech. **46** (1971) 199
25. S Thutupalli, R. Seemann and S. Herminghaus, New J. Physics **13** (2011) 073021
26. I Pagonabarraga and I. Lopis, Soft Matter **9** (2013) 7174
27. S. Kim and S.J. Karrila, *Microhydrodynamics: Principles and Selected Applications* (Dover Publications Inc. Mineola, New York 2005)
28. C. Pozrikidis, *Boundary integral and singularity methods for linearized viscous flow.* (Cambridge University Press 1992)
29. I.M. Zaid, J. Dunkel and J.M. Yeomans, J. Royal Society Interface **8** (2011) 1314
30. K.C. Leptos, J.S. Guasto, J.P. Gollub, A.I. Pesci and R.E. Goldstein, Phys. Rev. Lett. **103** (2009) 198103
31. I. Rushkin, V. Kantsler and R.E. Goldstein, Phys. Rev. Lett. **105** (2010) 188101
32. Z. Lin, J-L Thiffeault and S. Childress, J. Fluid Mech. **669** (2011) 167
33. D.O. Pushkin, H. Shum and J.M. Yeomans, J. Fluid Mech. **726** (2013) 5
34. P.T. Underhill, J.P. Hernandez-Ortiz and M.D. Graham, Phys. Rev. Lett. **100** (2008) 248101
35. D.T.N. Chen, A.W.C. Lau, L.A. Hough, M.F. Islam, M. Goulian, T.C. Lubensky, A.G. Yodh, Phys. Rev. Lett. **99** (2007) 148302
36. C. Darwin, Math. Proc. Cambridge Philosophical Society **49** (1953) 342
37. A.M. Leshansky and L.M. Pismen, Phys. Rev E **82** (2010) 025301
38. H. Kurtuldu, J.S. Guasto, K.A. Johnson and J.P. Gollub, PNAS **108** (2011) 10391
39. R. Golestanian and S. Ramaswamy (Eds.), European Physical Journal E **36** (Special Issue, Active Matter, 2013)
40. A.P. Berke, L. Turner, H.C. Berg and E. Lauga, Phys. Rev. Lett. **101** (2008) 038102
41. K. Drescher, J. Dunkel, L.H. Cisneros, S. Ganguly and R.E. Goldstein, PNAS **108** (2011) 10940
42. H.C. Fu, V.B. Shenoy and T.R. Powers, EPL **91** 24002 (2010)
43. R. Ledesma-Aguilar and J.M. Yeomans, Phys. Rev. Lett. **111** (2013) 138101